Supporting Information

Electric field-based ionic control of selective separation layers

Yan Zhao,[a, 1] Yanling Liu,[a, b, 1] Chao Wang,[c] Emily Ortega,[a, d] Xiaomao Wang,[b] Yuefeng F. Xie,[b] Jiangnan Shen,[c, *] Congjie Gao,[c] Bart Van der Bruggen[a, e, *]

[a]Department of Chemical Engineering, KU Leuven, Celestijnenlaan 200F, B-3001 Leuven, Belgium.

[b]State Key Joint Laboratory of Environment Simulation and Pollution Control, School of Environment, Tsinghua University, Beijing 100084, China.

[c]Center for Membrane Separation and Water Science & Technology, Ocean College, Zhejiang University of Technology, Hangzhou 310014, P. R. China.

[d]Department of Biological Sciences, University of Wisconsin-Milwaukee, Milwaukee, WI, 53201, United States.

[e]Faculty of Engineering and the Built Environment, Tshwane University of Technology, Private Bag X680, Pretoria 0001, South Africa.

[1]These authors contributed equally: Yan Zhao and Yanling Liu.

*Corresponding author: Jiangnan Shen shenjn@zjut.edu.cn

Bart Van der Bruggen bart.vanderbruggen@kuleuven.be

This PDF file includes:

Texts S1 to S4

Fig. S1 to S16

Table S1

References (11)

CONTENT

1. Theories.

1.1. Quantum mechanics mechanisms of ions in electric field.

The quantum state of microparticle/ion can be described by the wave function $\varphi(\vec{\mathbf{r}},\mathrm{t})$, Which is the Schrödinger equation.

$$\mathrm{i}\hbar\frac{\partial}{\partial t}\varphi(\vec{\mathrm{r}},\mathrm{t}) = (-\frac{\hbar^2}{2\mathrm{m}}\nabla^2 + \mathrm{V})\varphi(\vec{\mathrm{r}},\mathrm{t})$$

where m is the weight of microparticle/ion; $\hbar$ is the reduced Planck constant, which is 1.054571800*10^{-34} J·s. The ∇ is the gradiant operator, which is

$$\hat{\mathrm{p}} = -\mathrm{i}\hbar\vec{\nabla}$$

$\hat{\mathrm{p}}$ is the momentum operation

$$\overline{\vec{\mathrm{P}}} = \int \varphi^*(\vec{\mathrm{r}})\,\hat{\mathrm{p}}\varphi(\vec{\mathrm{r}})\mathrm{d}^3\mathrm{x}$$

The general state of free microparticle/ion is a formation of a wave packet, which is the superposition of many plane monochromatic waves.

$$\mathrm{i}\hbar\frac{\partial}{\partial t}\varphi(\vec{\mathrm{r}},\mathrm{t}) = -\frac{\hbar^2}{2\mathrm{m}}\nabla^2\varphi(\vec{\mathrm{r}},\mathrm{t})$$

$$\varphi(\vec{\mathrm{r}},\mathrm{t}) = \frac{1}{(2\pi\hbar)^{3/2}}\int_{-\infty}^{+\infty}\varphi(\vec{\mathrm{p}})\exp[\mathrm{i}(\vec{\mathrm{p}}\cdot\vec{\mathrm{r}} - \mathrm{Et})/\hbar]\mathrm{d}^3\mathrm{p}$$

due to the relationship between the energy E and the momentum $\vec{\mathrm{p}}$

$$\mathrm{E} = \frac{\vec{\mathrm{p}}^2}{2\mathrm{m}}$$

When the potential field excluding the time t, then

$$\varphi(\vec{\mathrm{r}},\mathrm{t}) = \varphi(\vec{\mathrm{r}})\mathrm{f}(\mathrm{t})$$

thus,

$$\varphi(\vec{\mathrm{r}}) = \frac{1}{(2\pi\hbar)^{3/2}}\int_{-\infty}^{+\infty}\varphi(\vec{\mathrm{p}})\exp[\mathrm{i}(\vec{\mathrm{p}}\cdot\frac{\vec{\mathrm{r}}}{\hbar})\mathrm{d}^3\mathrm{p}$$

which means once the $\varphi(\vec{\mathrm{r}})$ is a determined value, the distribution probabilities of observed values of the mechanical quantity are ensured, which can be used to describe the three dimensional microparticle/ion state. The superposition of states theory is described by the coherent superposition of waves and the wave function (The state of

the microscopic system).

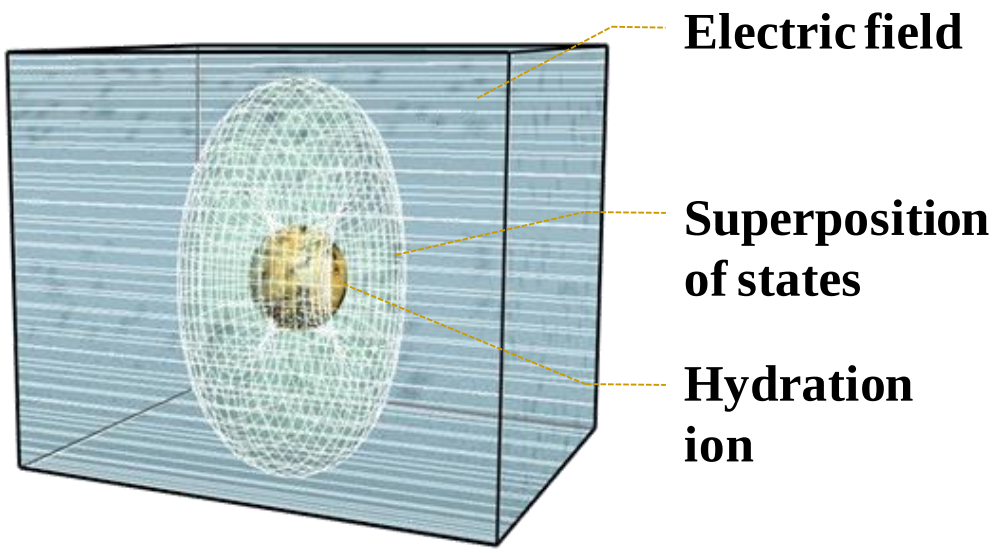

Fig. S1 Scheme of superposition states of ions affected by the electric field, other charged groups or ions and the target membrane layer itself.

2.2. Hydration ion.

Usually, ions in water are in hydrated conditions, which play an important role in the physical and chemical processes.

The hydrated ion consists three parts, the ion of the core, coordination water molecule of the coordination-solvent mixing zone and the non-coordination water molecule of the random change zone. As shown in Fig. S2, the hydrated ionic diameter is the diameter contain with ion, coordination-solvent zone and the random change zone.

In the coordination-solvent mixing zone, water molecules form coordination bonds with the ion, the number of these water molecules (C_N) is calculated

$$C_N = \frac{(r_{M^z} + r_{H_2O})^3}{r_{M^z}^3}$$

where r_{M^z} is the radius of ion; r_{H_2O} is the radius of water molecular and z is the valence number of ions.

In the random change zone, water molecules not form the coordination bonds with ions, the number of these part of water molecules is also called solvent number

of water molecules (S_N)

The totally ionic hydrated energy ΔG was calculated by

$$\Delta G = U_c + U_s + U_r + U_h + U_p$$

In this process, the U_c is the energy of C_N and calculated by

$$U_c = \frac{N_A \cdot e^2 \cdot Z^2}{\varepsilon \cdot r_{M^{z+}}} \cdot (C_N)$$

U_s is the energy of C_N and was calculated by

$$U_s = 13.2 \cdot \frac{Z^2}{r^2_{M^{z+}}} \cdot (S_N)$$

where e is the quantity of electric charge; ε is the dielectric constant; the N_A is the Avogadro constants.

U_r is the rotational energy of water molecules in coordination-solvent mixing zone.

$$U_r = \frac{n \cdot i}{2RT}$$

$$U_r' = \frac{U_r}{n \cdot N_A}$$

$$\overline{U_r} = \frac{i}{2KT}$$

where n is the molar weight; i is the rotational degrees of freedom of water molecule; R is the thermodynamic parameters; T is the thermodynamic temperature; U_r' is the rotational energy of each water molecule in coordination-solvent mixing zone; $\overline{U_r}$ is the average rotational energy of water molecules in coordination-solvent mixing zone. the Boltzmann constant is

$$K = \frac{R}{N_A}$$

U_h is the hydrogen bond energy and each of the hydrogen bond energy is about 18.81kJ·mol^{-1} and the number of hydrogen bond (HBN) in the Coordination-Solvent mixing Zone could be calculated by

$$HBN = (C_N) - Z$$

U_p is the Polarization energy of water molecules, which in the random change zone and was calculated by

$$U_p = \frac{\alpha \cdot (Z^*)^2}{r_{Mz+}}$$

where Z* is the effective relative permittivity. α is a constant and related to the electronic configurations.

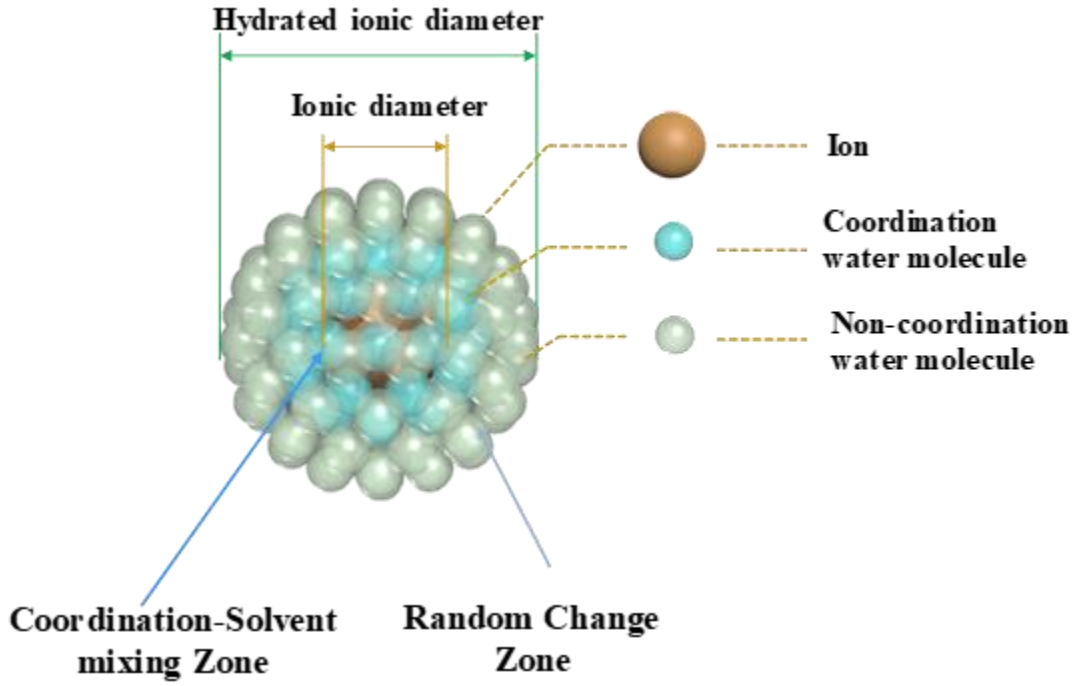

Fig. S2 The scheme of the hydrated ion.

2.3. Alternating current layer-by-layer assembly technology

The layer-by-layer (LbL) assembly technogy have been applied for preparation of multilayer of membranes and achieved highly efficient selectivity performances. Combined with the electric field force, the polymers or monomers, which are mixed into the waters, are LbL assembly on membrane surface. The alternating current LbL assembly technology with the specific alternating current frequency can be design and used to fabricate the multilayer on membrane surface. As shown in Fig. S3, under the alternating current field, the polyelectrolytes are selectivity assembled as a high frequency. When the direction of electro field force is consistent with the electric force (the interaction force between membrane surface and charged materials), the

charged materials will move and cover on the membrane surface. In this process, the inevitable of these materials stack on the surface. However, once the direction is opposite, especially for the stacked and instable materials, they will fall form the surface. Thus, in this alternating current LbL assembly process, the polyelectrolytes/changed monomers are selectively coated on membrane surface. Only the stable of the polyelectrolytes/changed monomers can be assembled on the surface and the redundant polyelectrolytes/changed monomers can not exist in the multilayer structure so that formed a homogeneous multilayer structure.

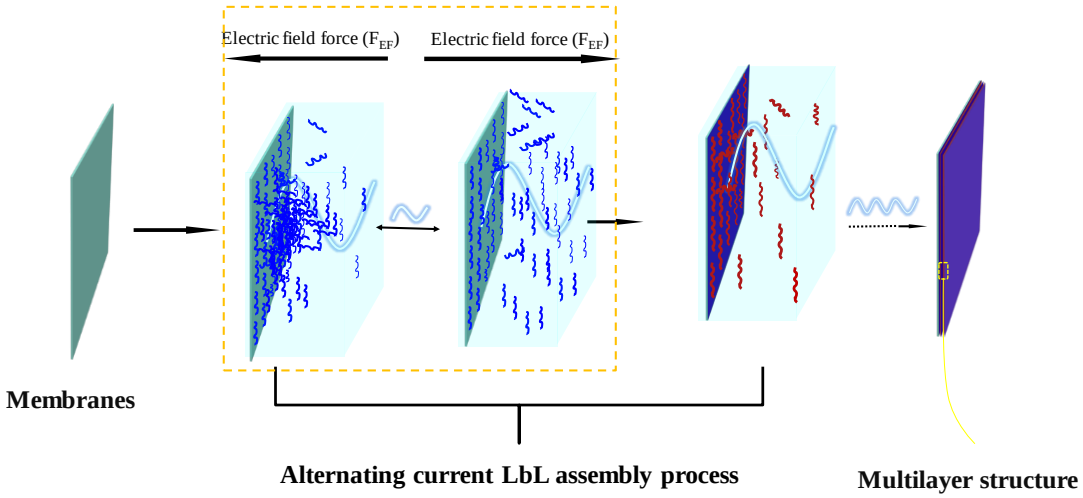

Fig. S3 The technology of the alternating current layer-by-layer assembly for membrane preparation.

2. Materials.

2.1. Chemicals

L-dopa, 4-amino-benzenesulfonic acid monosodium salt (ABS), dopamine, 2,3-epoxypropyl trimethyl ammonium chloride (ETAC), tris(dimethylaminomethyl)phenol (DMP30), tris-(hydroxymethyl)aminomethane (Tris-HCl), cupric sulfate ($CuSO_4$), hydrogen peroxide (H_2O_2), 1-ethyl-3-(3-dimethylami-nopropyl) carbodiimide hydrochloride (EDC-HCl), N-hydroxy succinimide (NHS), sodium bromide (NaBr), sodium chloride (NaCl), sodium sulfate (Na_2SO_4), sodium phosphate (Na_3PO_4), potassium chloride (KCl), lithium chloride (LiCl), magnesium chloride ($MgCl_2$), calsium chloride ($CaCl_2$) and all other chemicals were obtained from Sigma-Aldrich (Germany). 2-Hydroxypropyltrimethyl ammonium chloride chitosan (HACC) (M_W = 20,000 g/mol) was obtained from Cool Chemical Science and Technology Co., Ltd (China). Poly(4-styrenesulfonic acid-co-maleic acid) sodium salt (PSSMA) (M_W = 20,000 g/mol) was obtained from Sigma-Aldrich (Germany). All other chemicals were obtained from Sigma-Aldrich (Germany) and all the chemicals were used without any further purification.

2.2. Commercial ion exchange membranes

In this work, the Fujifilm commercial anion exchange membrane (Type I) and cation exchange membrane (Type I) were selected and modified; the data were shown in Table S1. Fujifilm’s customized membranes are based on new polymer technology in combination with thin substrates. The homogeneous Fujifilm ion exchange membranes are applicable in various applications.

Table S1. The data of commercial membranes.*

Product Name	Type	Thickness/μm	Surface electric resistance/Ω·m^2	Brust strength/kPa
CEM-0.0	Cation exchange membrane	135	1.3 in 2.0 M NaCl	2.4 (wet)
AEM-0.0	Anion exchange membrane	125	0.8 in 2.0 M NaCl	2.7 (wet)

*Data from manufactures.

2.3. Chemical structures.

2.3.1 Preparation of multilayer surface for anion exchange membranes.

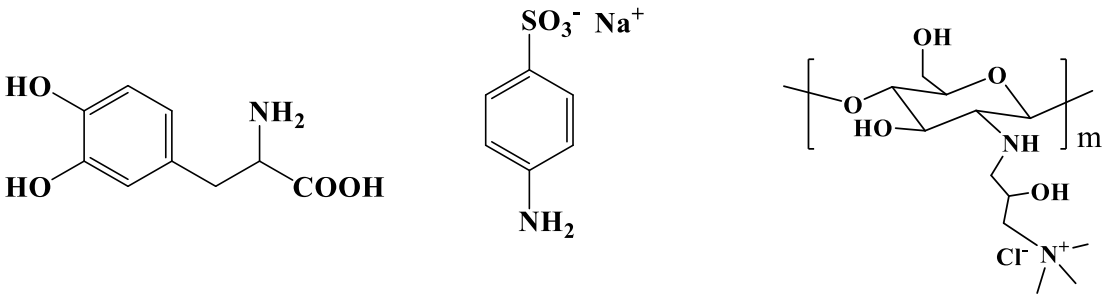

L-dopa **ABS** **HACC**

Fig. S4 The chemical structure of L-dopa, ABS and HACC.

2.3.2 Preparation of multilayer surface for cation exchange membranes.

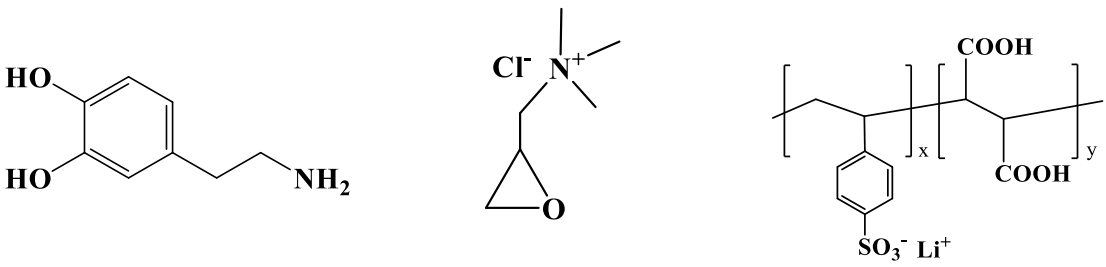

Dopamine **ETAC** **PSSMA**

Fig. S5 The chemical structure of dopamine, ETAC and PASSMA.

3. Experimental section

3.1. Cl^- control membrane surface multilayers on AEM surface.

The commercial anion exchange membranes (AEM-0.0) were cleaned by pure water and stored in 0.10 M NaCl solution for 24 h. Then, the membrane surfaces were cleaned by pure water.

The membranes were placed vertically into a device, which is an experimental alternating current assembly technology device for membrane preparation.

Firstly, 0.30 g L-dopa and 1.755 g NaCl were added into the 150 mL of Tris-HCl (pH=8.5) solution, using $CuSO_4$ as a trigger, the color of the solution changed from blue to light green (Preparation of the standard Tris-HCl, $CuSO_4$ solution: 10 mM Tris-HCl were prepared and the solution should keep the pH = 8.8 by using 1 M HCl. Then, 5 mM Cu_2SO_4 was mixed into the solution). Once the L-dopa and NaCl dissolved into the solution, 0.30 mL H_2O_2 was added into the mixed solution and added into the device immediately. At the same time, the electric field was provided by a programmable alternating current power supply (PPS 1005) (EVERFINE Instrument Co., Ltd. China). An effective alternating current voltage of 10 V was chosen, and the frequency was 50Hz (400 mL 0.2 M NaCl solution was chose as the electrode solution) and the mechanical stirring was kept at 300 rpm. The color changed rapidly from light green to dark green, from dark green to light brown, and slowly from light brown to dark brown.

4 h later, removed all the solutions and measured the membrane surface by pure water for 3 times. Then, 150 mL of the solution with 4 $g \cdot L^{-1}$ ABS and 0.2 M NaCl was added into the device, Keeping the effective alternating current voltage of 10 V and the frequency was 50Hz (400 mL 0.2 M NaCl solution was chose as the electrode solution) and the mechanical stirring was kept at 300 rpm. Besides, 100 mg EDC-HCl and 60 mg NHS were added at the same time.

12 h later, the reaction was finished. Rremoved all the solutions and cleaned the membrane surface by pure water for 3 times. Then, the resulting AEM with 0.5 bilayer was obtained, which named as AEM-0.5.

Secondly, 150 mL mixing solution with 2 $g \cdot L^{-1}$ HACC and 0.2 M NaCl was added into the device. The electric field was provided by a programmable alternating

current power supply immediately. The effective alternating current voltage of 10 V was chosen, and the frequency was 50Hz (400 mL 0.2 M NaCl solution was chose as the electrode solution) and the mechanical stirring was kept at 300 rpm.

30 min later, the reaction was finished. Rremoved all the solutions and cleaned the membrane surface by pure water for 3 times. Then, the resulting AEM with 0.5 bilayer was obtained, which named as AEM-1.0.

Repeated the above steps and obtained the AEM-0.5, AEM-1.5, AEM-3.5, and AEM-5.5, and immersed the resulting membranes into the pure water at room temperature (about 25 ^{o}C).

3.2. Li^{+} control membrane surface multilayers on CEM surface.

The commercial cation exchange membranes (CEM-0.0) were cleaned by pure water and stored in 0.10 M LiCl solution for 24 h. Then, the membrane surfaces were cleaned by pure water.

The membranes were placed vertically into a device, which is an experimental alternating current assembly technology device for membrane preparation.

Firstly, 0.30 g dopamine and 1.65 g Li_2SO_4 were added into the 150 mL of Tris-HCl (pH=8.5) solution, using $CuSO_4$ as a trigger, the color of the solution changed from blue to light brown (Preparation of the standard Tris-HCl, $CuSO_4$ solution: 10 mM Tris-HCl were prepared and the solution should keep the pH = 8.8 by using 1 M HCl. Then, 5 mM Cu_2SO_4 was mixed into the solution). Once the dopamine and Li_2SO_4 dissolved into the solution, 0.30 mL H_2O_2 was added into the mixed solution and added into the device immediately. At the same time, the electric field was provided by a programmable alternating current power supply (PPS 1005) (EVERFINE Instrument Co., Ltd. China). An effective alternating current voltage of 10 V was chosen, and the frequency was 50Hz (400 mL 0.1 M Li_2SO_4 solution was chose as the electrode solution) and the mechanical stirring was kept at 300 rpm. The color changed from light to black.

4 h later, removed all the solutions and measured the membrane surface by pure water for 3 times. Then, 150 mL of the solution with 1 mL DMP30, 5 mL ETCA and 0.1 M Li_2SO_4 was added into the device, Keeping the effective alternating current voltage of 10 V and the frequency was 50Hz (400 mL 0.1 M Li_2SO_4 solution was

chose as the electrode solution) and the mechanical stirring was kept at 300 rpm.

30 min later, the reaction was finished. Rremoved all the solutions and cleaned the membrane surface by pure water for 3 times. Then, the resulting CEM with 0.5 bilayer was obtained, which named as CEM-0.5.

Secondly, 150 mL mixing solution with 2 $g \cdot L^{-1}$ PSSMA and 0.1 M Li_2SO_4 was added into the device. The electric field was provided by a programmable alternating current power supply immediately. The effective alternating current voltage of 10 V was chosen, and the frequency was 50 Hz (400 mL 0.1 M Li_2SO_4 solution was chose as the electrode solution) and the mechanical stirring was kept at 300 rpm.

30 min later, the reaction was finished. Rremoved all the solutions and cleaned the membrane surface by pure water for 3 times. Then, the resulting CEM with 0.5 bilayer was obtained, which named as CEM-1.0.

Repeated the above steps and obtained the CEM-0.5, CEM-1.5, CEM-3.5, and CEM-5.5, and immersed the resulting membranes into the 100 mg EDC-HCl and 60 mg NHS mixing solution in the device. 24 h later, the membrane surface was washed by pure water and stored in the pure water at room temperature (about 25 ^{o}C).

3.3. Membrane surface electric resistance measurement.

The membrane surface electrical resistance was measured in 0.50 M NaCl. 0.2 M 0.2 M Na_2SO_4 was chosen as the electrode solution. As shown in Fig. S6, the surface electrical resistance R_{SER} ($\Omega \cdot cm^2$) was calculated as

$$R_{SER} = \frac{U - U_0}{I} \times S$$

where U is the voltage of the membrane samples and U_0 is the voltage of the blank expressed in V, I is the constant current through the membranes, which was 0.04 A. S is the effective area of the membrane, which was 7.065 cm^2.

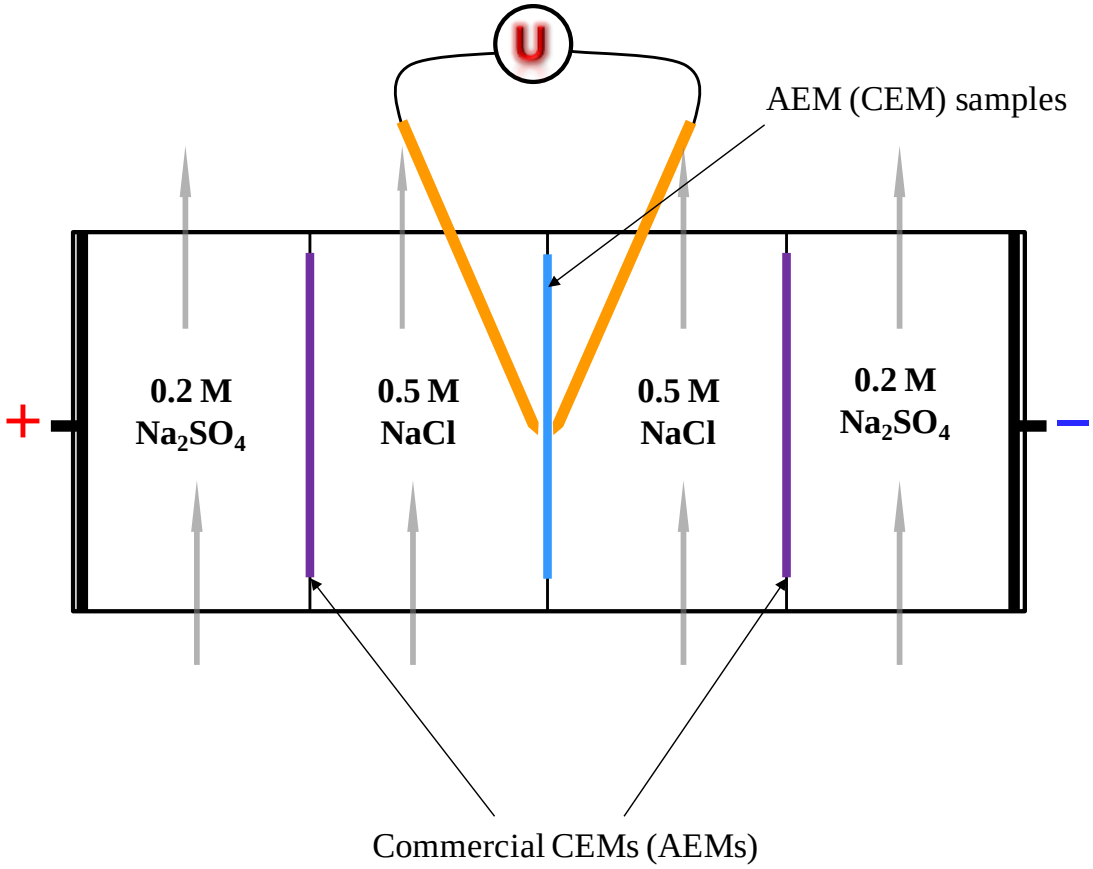

Fig. S6 Scheme of the membrane surface electric resistance measurement.

3.4. Current-voltage curves measurement.

The polarization current voltage curves were measured in a four-electrode mode under incremental direct current to characterize the electrochemical behavior of the modified membranes. 0.1 M NaCl and 0.2 M Na_2SO_4 were used as test solution and electrode solution respectively. The effective area of membrane was 7.065 cm^2, as shown in Fig. S7.

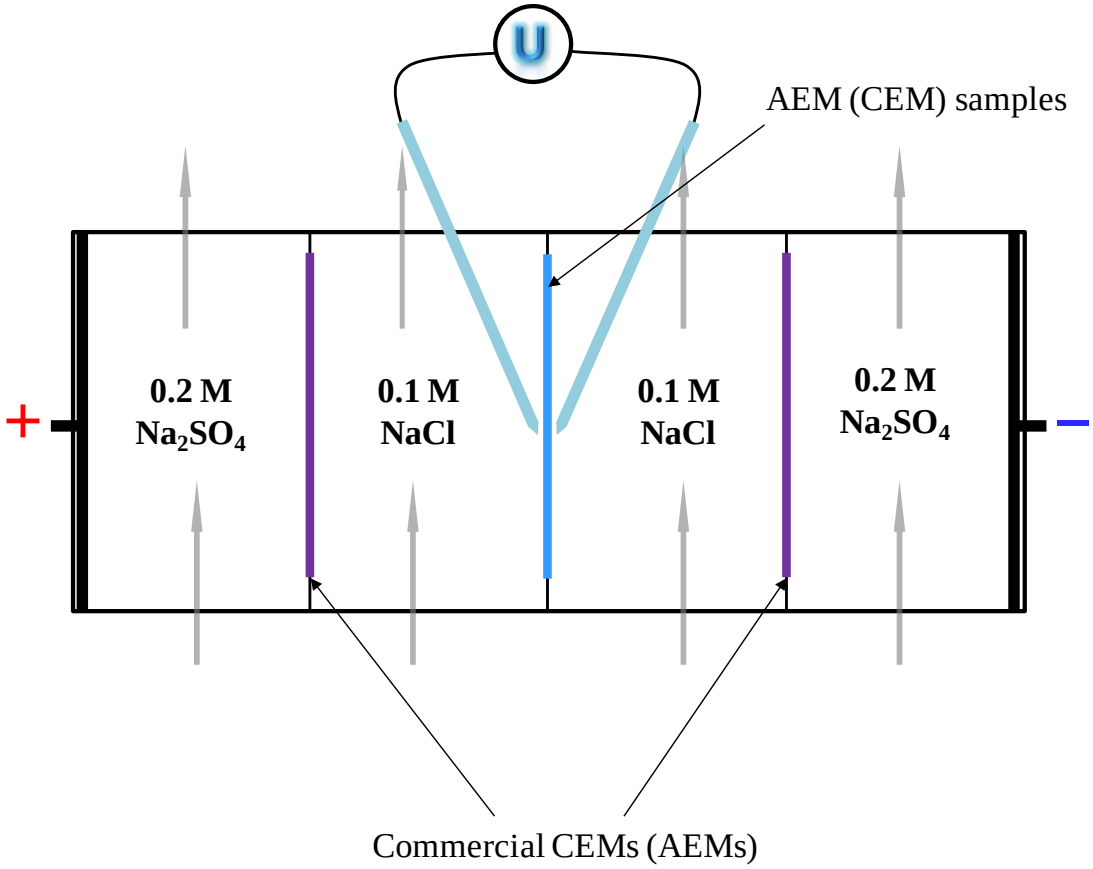

Fig. S7 Scheme of the membrane current-voltage curves measurement.

3.5. Selective separation measurement for anion exchange membrane.

The temporal evolution of PO_4^{3-} (multivalent anion), SO_4^{2-} (multivalent anion), Cl^- (monovalent anion) and Br^- (monovalent anion) concentrations in ED was measured to evaluate the selective separation of PO_4^{3-}/ SO_4^{2-}/ Cl^-/ Br^-. The initial composition of feed solutions both in dilute and concentrated compartments are 50 mM Na_3PO_4, Na_2SO_4, NaCl and NaBr solutions. In this process, the effective area of membrane was 20.0 cm^2 and the application of constant current was 0.20 A, which the membrane surface current was 10 $mA \cdot cm^{-1}$. The electrode solution was 300 mL 0.2 M Na_2SO_4. Every 10 min, the concentration of PO_4^{3-}, SO_4^{2-}, Cl^- and Br^- in dilute were tested by ion chromatography.

3.6. Selective separation measurement for anion exchange membrane.

The temporal evolution of Mg^{2+} (multivalent cation), Ca^{2+} (multivalent cation), Li^{+} (monovalent cation) and K^{+} (monovalent cation) concentrations in ED was measured to evaluate the selective separation of Mg^{2+}/ Ca^{2+}/ Li^{+}/ K^{+}. The initial composition of feed solutions both in dilute and concentrated compartments are 50 mM $MgCl_2$, $CaCl_2$, LiCl and KCl solutions. In this process, the effective area of membrane was 20.0 cm^2 and the application of constant current was 0.20 A, which the membrane surface current was 10 $mA \cdot cm^{-1}$. The electrode solution was 300 mL 0.5 M NaCl. Every 10 min, the concentration of Mg^{2+}, Ca^{2+}, Li^{+}, K^{+} in dilute were tested by ion chromatography.

3.7. The selective separation efficiency parameter.

The selective separation efficiency parameter is applied to illustrate the selective separation efficiency between the two kinds of ions. When the selective separation efficiency is lower than zero, it indicates that no selective separation between the two components. Otherwise, when the selective separation efficiency is higher than zero, it suggests selective separation of two ions. The selective separation efficiency between component A and B is calculated as,

$$S(t) = \frac{((c_A(t))/(c_A(0))) - ((c_B(t))/(c_B(0)))}{(1 - (c_A(t))/(c_A(0))) + (1 - ((c_B(t))/(c_B(0)))} \times 100\%$$

where $c_A(0)$ and $c_B(0)$ are the initial concentration of component A and B, respectively; $c_A(t)$ and $c_B(t)$ are the concentration of component A and B at time t.

3.8. The permselectivity of ions.

The permselectivity (P_A^B) of the ion exchange membranes is used to show the rate of transport between two kinds of ions. When the permselectivity lower than 1, it indicates that no selective separation for two components. Otherwise, when the permselectivity is higher than 1, it suggests selective separation between the two ions. P_A^B (Between component A and B) was calculated,

$$P_A^B = \frac{t_B/t_A}{c_B/c_A} = \frac{J_B \cdot c_A}{J_A \cdot c_B}$$

where t_A and t_B are the transport number o of component A and B. J_A and J_B are the ion flux and expressed in eq./m^2·s and the flux of ions (J_i) was calculated according to

$$J_i = \frac{V \cdot \frac{dc_i}{dt}}{A}$$

where V is the volume of solution and A is the active area.

3.9. Scanning electronic microscopy (SEM), energy dispersive x-ray spectroscopy (EDS).

The morphologies and structures of all the membrane samples (surface and cross-sectional) were characterized by using scanning electronic microscopy (SEM, Hitachi S-4800) at an accelerating voltage of 10.0 kV. The EDS maps C, O, N and S element of the membrane cross-sectional were provided at the same time.

3.10. Atomic force microscope (AFM).

Atomic force microscopy (AFM, Bruker, United States) equipped with a noncontact type scanner was used to acquire membrane surface three dimensional topography. These images were captured under tapping mode at room temperature (25°C). The scanning area of membrane surface is a 2 μm × 2 μm of each sample.

3.11. X-ray photo-electron spectroscopy (XPS).

The elemental compositions of the membrane samples (membrane surface) were characterized by X-ray photo-electron spectroscopy (XPS, Kratos AXIS Ultra DLD, Japan). The anode was mono (Al (Mono)) (45 W). The charge neutralizer was on

current 1.8 A, balance 3.3 V and bias 1.0 V.

3.12. Attenuated total reflection Fourier transforms infrared (ATR-FTIR).

The total reflectance Fourier transform infrared spectroscopy (ATR-FTIR, Nicolet 6700, United States) was used to monitored the functional groups of membrane samples (membrane surface). Membranes were dried thoroughly in vacuum oven at 60 ℃ for 8 h before measurements.

4. Results and analysis

4.1. SEM images of anion exchange membranes.

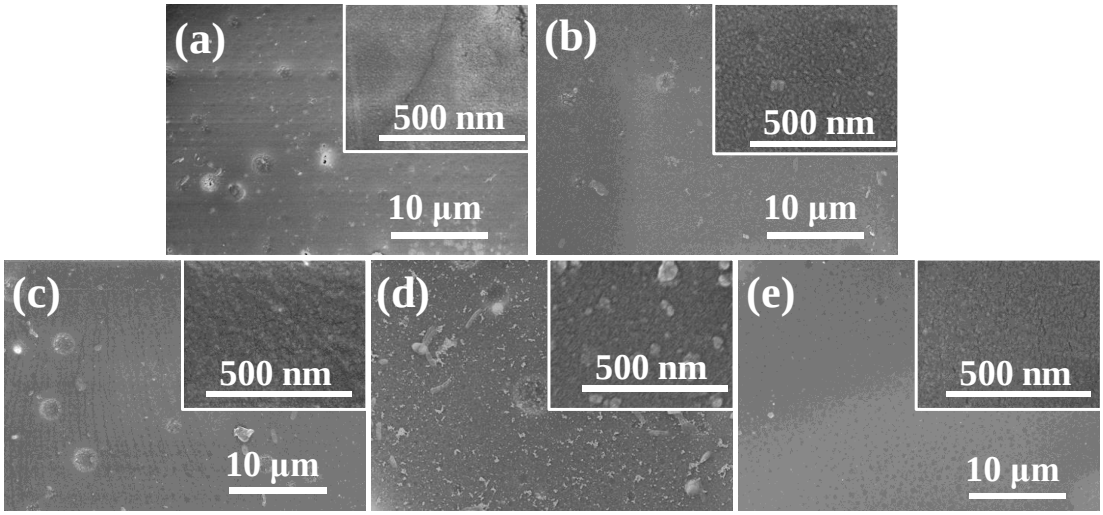

Fig. S8 Surface SEM images of AEM-0.0 (a), AEM-0.5 (b), AEM-1.5 (c), AEM-3.5 (d) and AEM-5.5 (e).

4.2. SEM images of cation exchange membranes.

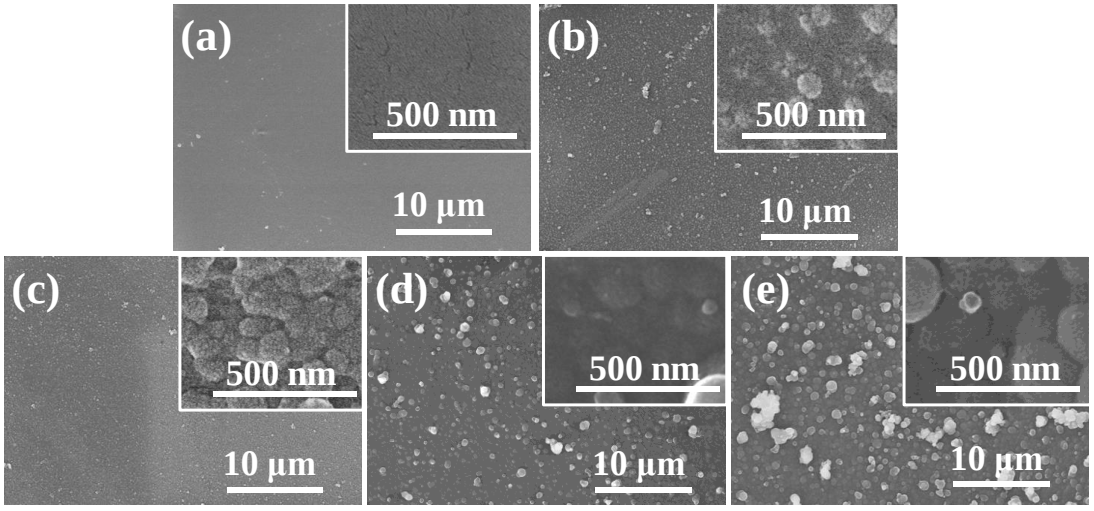

Fig. S9 Surface SEM images of CEM-0.0 (a), CEM-0.5 (b), CEM-1.5 (c), CEM-3.5 (d) and CEM-5.5 (e).

4.3. AFM images of anion exchange membranes.

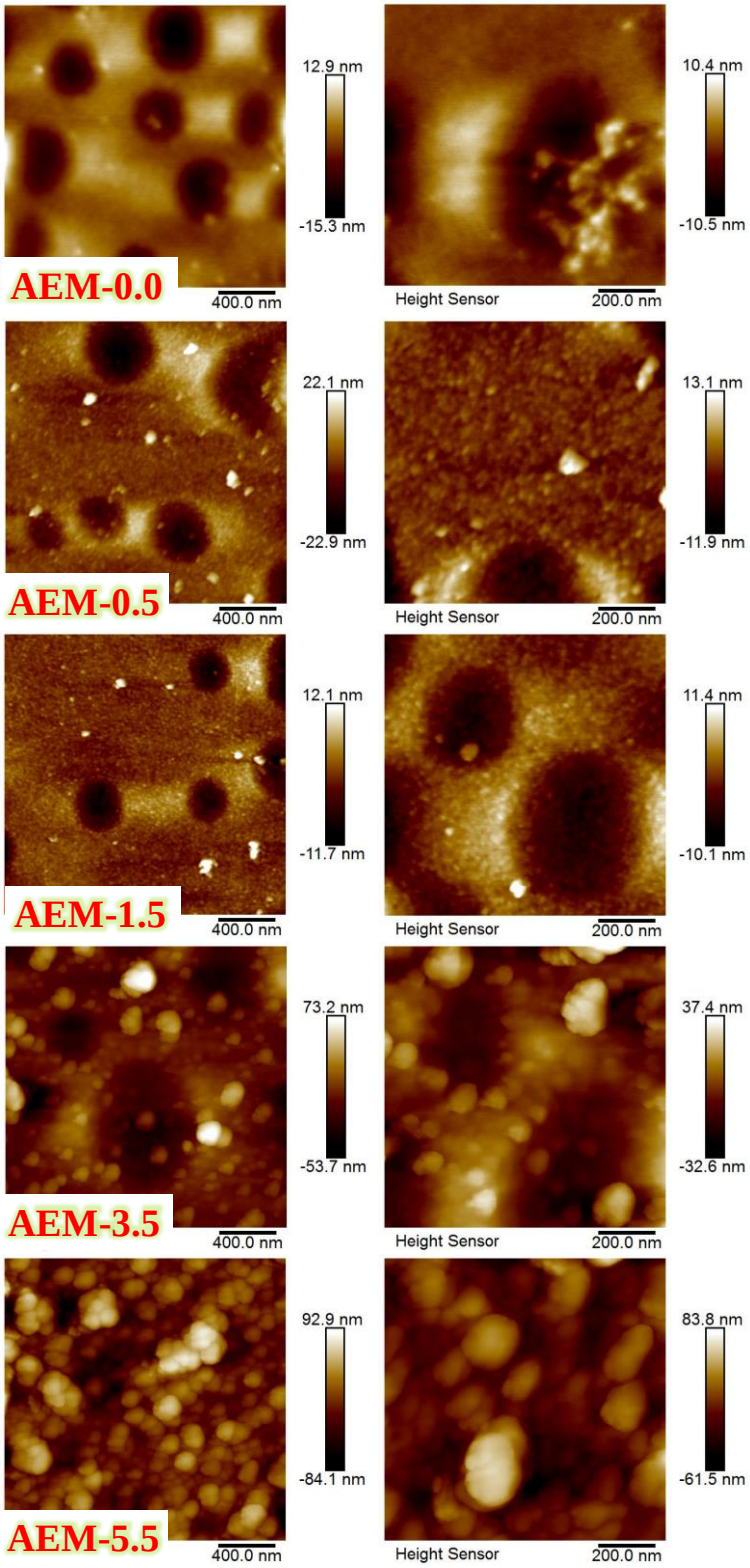

Fig. S10 The AFM images of AEM-0.0, AEM-0.5, AEM-1.5, AEM-3.5 and AEM-5.5.

4.4. AFM images of cation exchange membranes.

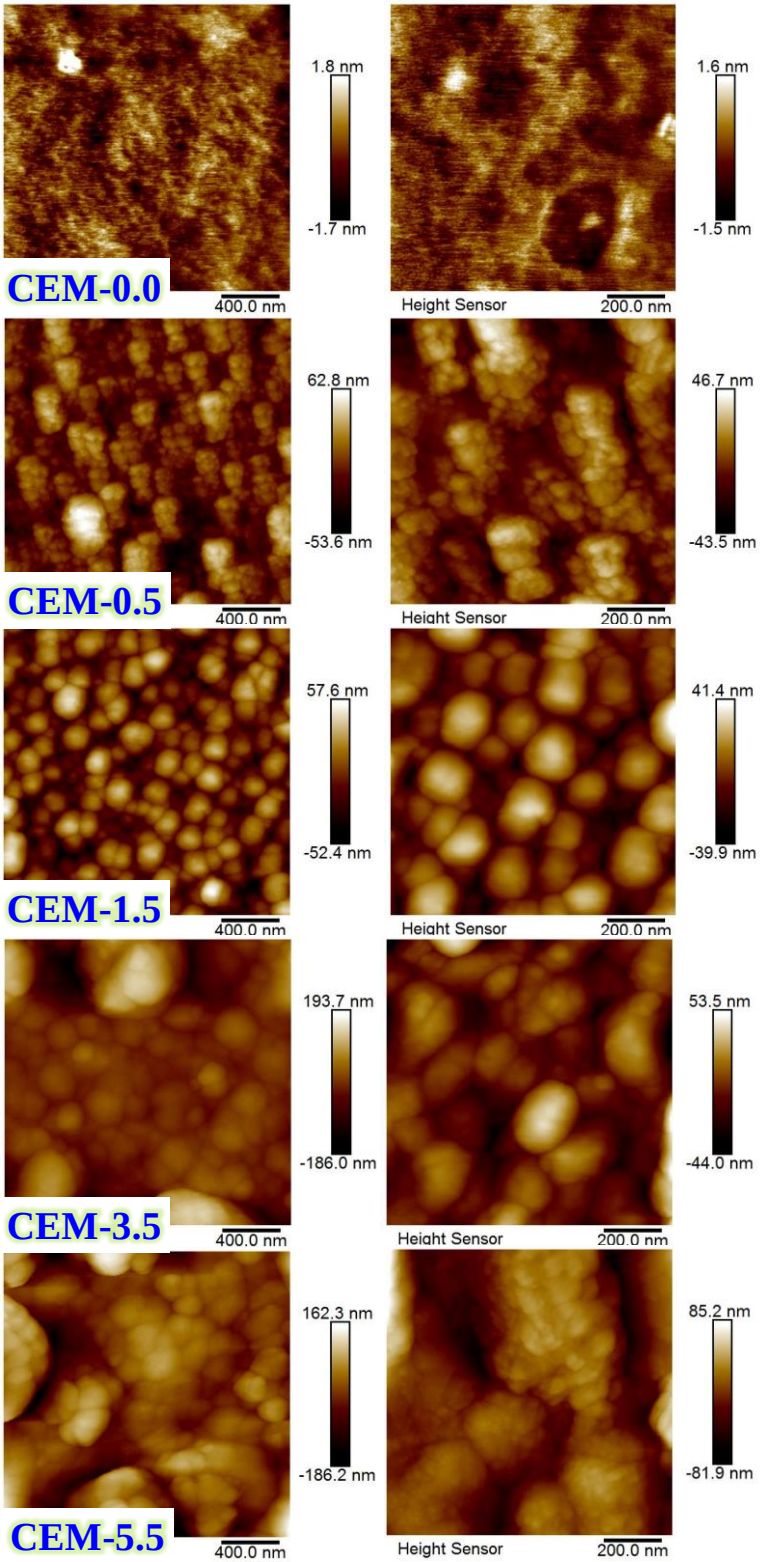

Fig. S11 The AFM images of CEM-0.0, CEM-0.5, CEM-1.5, CEM-3.5 and CEM-5.5.

4.5. The current-voltage curves of anion exchange membranes.

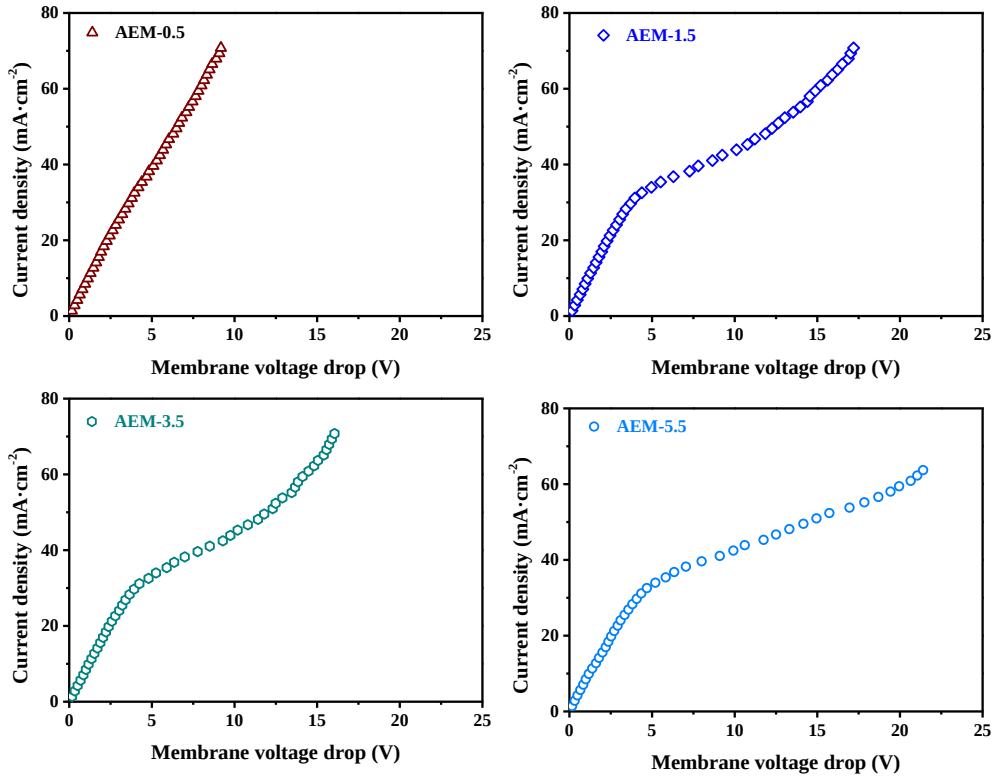

Fig. S12 The current-voltage curves of AEM-0.5, AEM-1.5, AEM-3.5 and AEM-5.5.

4.6. The current-voltage curves of cation exchange membranes.

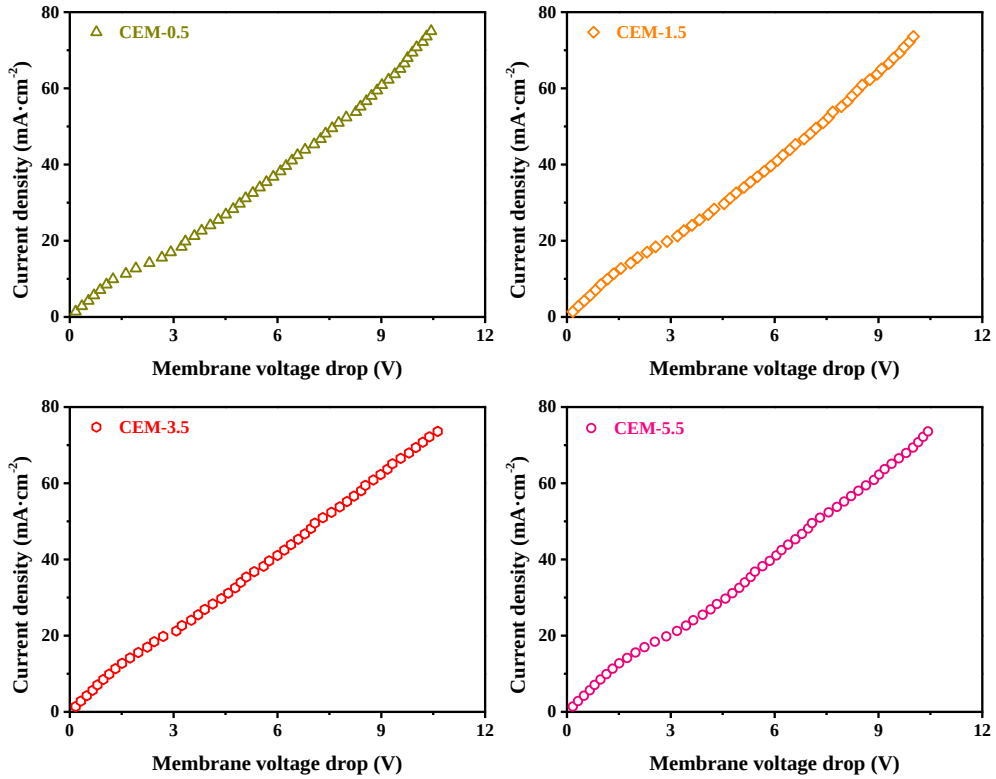

Fig. S13 The current-voltage curves of CEM-0.5, CEM-1.5, CEM-3.5 and CEM-5.5.

4.7. The current-voltage curves of ASV and CSO membranes.

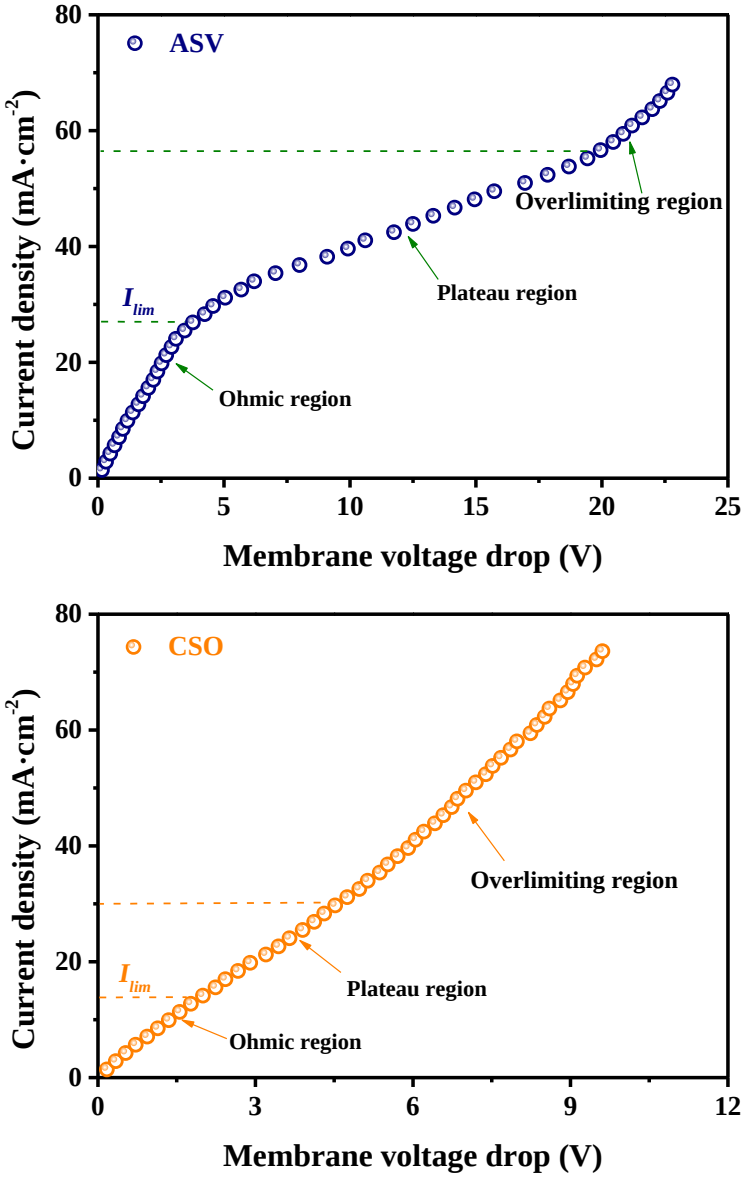

Fig. S14 The current-voltage curves of ASV and CSO.

4.8. The selective separation performance for Cl^-, Br^-, SO_4^{2-} and PO_4^{3-} of anion exchange membranes.

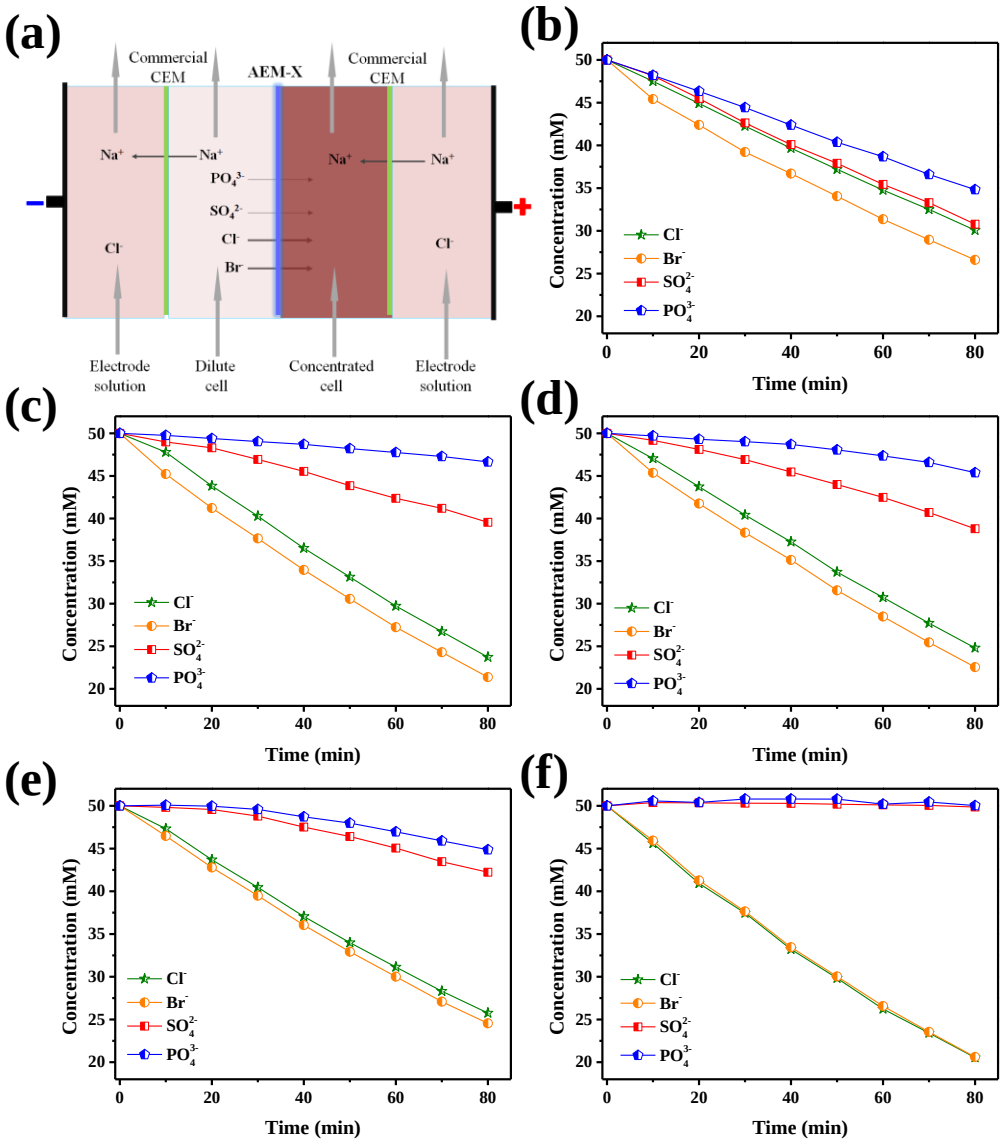

Fig. S15 Schematic of anions separation (a); the selective separation performance of Cl^-, Br^-, SO_4^{2-} and PO_4^{3-} by using AEM-0.0 (b), AEM-0.5 (c), AEM-1.5 (d), AEM-3.5 (e) and AEM-5.5 (f).

4.9. The selective separation performance for Li^+, K^+, Mg^{2+} and Ca^{2+} of anion exchange membranes.

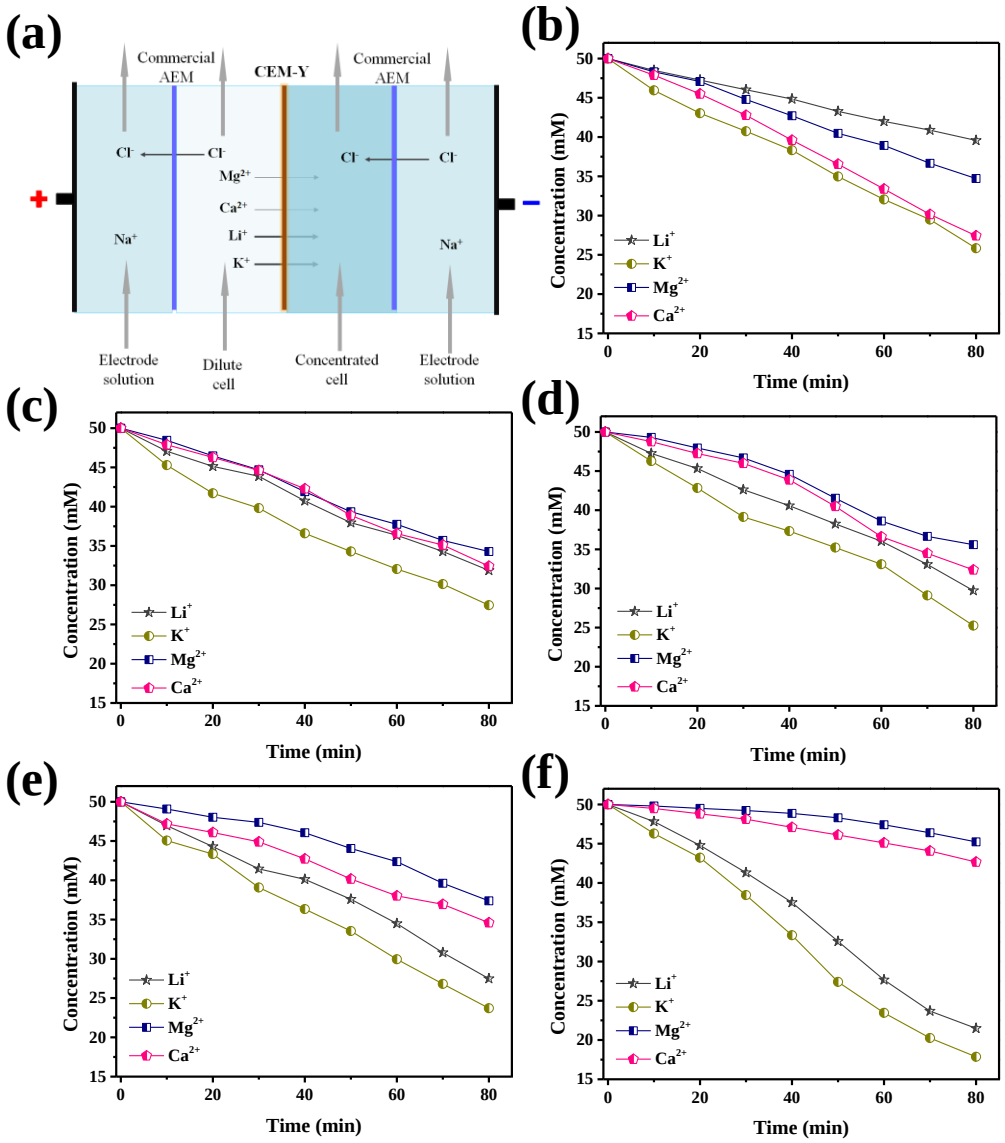

Fig. S16 Schematic of cation separation (a); the selective separation performance of Li^+, K^+, Mg^{2+} and Ca^{2+} by using CEM-0.0 (b), CEM-0.5 (c), CEM-1.5 (d), CEM-3.5 (e) and CEM-5.5 (f).

References

1. H. Che, S. Chen, Y. Xie, H. Wang, K. Amine, X.-Z. Liao and Z.-F. Ma, *Energ. Environ. Sci.*, 2017, **10**, 1075-1101.
2. Y. Guo, Y. Ying, Y. Mao, X. Peng, B. Chen, *Angew. Chem. Int. Edit.*, 2016, **55**, 15120-15124.
3. Y. Zhao, W. Shi, B. Van der Bruggen, C. Gao and J. Shen, *Adv. Mater. Interfaces*, 2018, **5**, 1701449.
4. Y. Zhao, C. Gao and B. Van der Bruggen, *Nanoscale*, 2019, **11**, 2264-2274.
5. Y. Zhao, Y. Li, J. Zhu, A. Lejarazu-Larranaga, S. Yuan, E. Ortega, J. Shen, C. Gao, B. Van der Bruggen, *J. Mater. Chem. A*, 2019, **7,** 13903–13909
6. Y. Zhao, Y. Li, S. Yuan, J. Zhu, S. Houtmeyers, J. Li, R. Dewil, C. Gao and B. Van der Bruggen, *J. Mater. Chem. A*, 2019, **7**, 6348-6356.
7. Y. Zhao, C. Zhou, J. Wang, H. Liu, Y. Xu, J. W. Seo, J. Shen, C. Gao and B. Van der Bruggen, *J. Mater. Chem. A*, 2018, **6**, 18859-18864
8. Y. Zhao, J. Zhu, J. Li, Z. Zhao, S. I. Charchalac Ochoa, J. Shen, C. Gao and B. Van der Bruggen, *ACS Appli. Mater. Interfaces*, 2018, **10**, 18426-18433.
9. M. Zhang, K. Guan, Y. Ji, G. Liu, W. Jin and N. Xu, *Nat. Commun.*, 2019, **10**, 1253.
10. C. Leighton, *Nat. Mater.*, 2019, **18**, 13-18.
11. Y. Zhang, Y. Wan, G. Pan, X. Wei, Y. Li, H. Shi and Y. Liu, *J. Membrane Sci.*, 2019, **573**, 11-20.